RSC Advances

PAPER

View Article Online
View Journal | View Issue

Cite this: *RSC Adv.*, 2023, **13**, 19164

Psidium guajava leaf extract mediated green synthesis of silver nanoparticles and its application in antibacterial coatings

Md. Johurul Islam,†[a] Nazia Khatun,†[a] Riyadh Hossen Bhuiyan,[b] Shahnaz Sultana,[c] Md. Aftab Ali Shaikh,[de] Md. Nur Amin Bitu,[a] Fariha Chowdhury[e] and Suravi Islam *[a]

In this study, *Psidium guajava* (*P. guajava*) leaf extract-assisted silver nanoparticles (AgNPs) were synthesized and their antibacterial activities were investigated. The synthesized green AgNPs were characterized by various analytical techniques including UV-Vis spectroscopy, Fourier transform infrared spectroscopy (FTIR), X-ray diffractometry (XRD), field emission scanning electron microscopy (FE-SEM), energy dispersive X-ray (EDX) spectroscopy, *etc.* From the UV-Vis spectroscopic analysis, the formation of nanoparticles has been confirmed by the color change from light yellow to reddish brown of the solution due to the excitation of the surface plasmon resonance peak at 430 nm. In addition, the FTIR study showed the reduction of Ag ions owing to the presence of biomolecules in the leaf extract, which acted as reducing as well as capping agents. Furthermore, XRD analysis reveals the identified 2θ peaks of AgNPs at ~39° with cubic structure. The FE-SEM micrograph illustrated the material was formed in nano-dimensions, with an average particle size of ~12 nm and almost spherical in shape. Moreover, *P. guajava*-mediated AgNPs demonstrated good antibacterial activity against both Gram-positive (*S. aureus*) and Gram-negative (*E. coli*) bacterial strains. The synthesis was performed by a bio-reduction process where a bioactive agent is responsible for reducing metallic ions to metallic nanoparticles as an eco-friendly, cost-effective, non-toxic, one-step, and sustainable method. Therefore, this study may create an imperative synthetic route for the fabrication of green-AgNPs and their application in antibacterial coatings in cotton textiles.

Received 21st May 2023
Accepted 20th June 2023

DOI: 10.1039/d3ra03381c

rsc.li/rsc-advances

1. Introduction

Nanotechnology is the most significant approach in modern scientific practice in the world. Researchers have made extensive development of electronics, environment and human health in medical science through nanotechnology.[1] The application of nanoparticles (NPs) in nanotechnology is increasing steadily.[2] To meet the demand, different synthesis methods are being created over time. Conventional (chemical or physical) methods are used as a complex method of making NPs which is harmful to the environment and human health due to chemical hazards and reaction contamination.[3,4] At the same time, conventional methods for synthesis of NPs are time-consuming, expensive, and toxic when handling.[5] On the other hand, green synthesis is eco-friendly and sustainable innovative method because various elements used here which come from organic materials.[6] Green synthesis of NPs is time saving and cost-effective bio-synthesis, with less chemical hazard. Metallic or oxide NPs, both are highly potential. This synthesis technique uses various elements which come from organic materials.[7–9]

Generally, wood and bones are used to produce NPs but in the green approach plants are popular more than others. Plants element likes bulks, roots, fruits and leaves are used typically to synthesize NPs.[10] Moreover, extract of green leaves of various medicinal plants are used as they have significant reducing and capping agents to convert metallic ions to form NPs. *Azadirachta indica* (neem), *Moringa oleifera*, *Justicia adhatoda*,[11] *Aloe vera* and *Psidium guajava* (*P. guajava*) *etc.* are common medicinal plants used for green synthesis of NPs. Among them, extract of *P. guajava* (guava) is used mostly because it contains glycosides and polyphenolics (flavonoids and tennies) which act as reducing and capping agents to convert metallic ions to NPs.[12–14] *P. guajava*, commonly known as guava, a popular fruit in

[a]*Industrial Physics Division, BCSIR Dhaka Laboratories, Bangladesh Council of Scientific and Industrial Research (BCSIR), Dhaka-1205, Bangladesh. E-mail: suraviislambcsir@gmail.com; suravii@yahoo.com*

[b]*Fibre and Polymer Research Division, BCSIR Dhaka Laboratories, Dhaka-1205, Bangladesh*

[c]*Institute of National Analytical Research and Service (INARS), BCSIR, Dhaka, Bangladesh*

[d]*Department of Chemistry, University of Dhaka, Dhaka-1000, Bangladesh*

[e]*Bangladesh Council of Scientific and Industrial Research (BCSIR), Dhaka-1205, Bangladesh*

† Contributed equally to this work.

Bangladesh. This evergreen tree is found throughout Asia and is widely cultivated in India, Bangladesh, and Malaysia.

Synthesis of various NPs such as Au, Cu, Ni, Al including Ag can be attained from guava leaf extract.[10,15,16] Several researchers have taken attempts to synthesize metallic nanoparticles exhausting aqueous extract of *P. guajava* leaves, especially silver nanoparticles considering wide range of advantages of green synthesis. Silver nitrate ($AgNO_3$) was used as a precursor and most of the research used (1–30) mM solution of silver ions reduced by different percentages of aqueous extract of *P. guajava* leaves. In the synthesis process silver salts, Ag^+ converts to metallic silver, Ag^0 through biological molecules of the leaf extract which may contain reducing agents as well as metal salt reducers. *P. guajava* leaf extract contains biochemicals such as polyphenols, carotenoids, terpenoids, flavonoids, tannins and triterpenes could be responsible for the reduction of metal ions to NPs.[9,10] Bose *et al.* prepared AgNPs using *P. guajava* and investigate their anti-bacterial activity against Gram negative bacterial strain.[9] Sharmila *et al.*[17] demonstrates result for both Gram-negative and Gram-positive bacteria with zone of inhibition less than 10 mm. Geetha *et al.* also get <10 mm inhibition zone by analyzing five pathogens for AgNP solutions.[18] Besides, Dama *et al.* prepared spherical AgNPs using methanol solvent and analyzed anti-microbial efficacy against *E. coli*, *S. aureus*, and *P. aeruginosa* microbes.[19] AgNPs has been applied in various fields such as engineering, communication, photochemical, bio-application, packaging antibacterial protection, *etc.* In addition, it has applications in biomedical devices, environmental remediation, medicine, food packaging, cosmetics, and other industrial purposes.[15]

AgNPs have distinct composition and structure, crystallinity, shape and size compared to the bulk forms. Consequently, it exhibited excellent physicochemical properties for instance chemical stability, surface-enhanced Raman scattering, high conductivity both thermal and electrical, catalytic activity, nonlinear optical behavior, and biological properties compare to others NPs.[16] AgNPs possess a wide-ranging spectrum of antibacterial and anti-fungal activities[14] generally applied to various consumer products for example cosmetics, toiletries, plastics, food, and textiles.[20]

The objective of this research is to synthesize eco-friendly AgNPs from *P. guajava* (myrtle family)[12] leaf extract and to examine its antibacterial activity. Here, synthesized AgNPs solutions with different concentrations of $AgNO_3$ were observed against Gram-negative bacteria to examine antibacterial activity. Finally, textile cotton and N95 mask fibers were coated with leaf extract-mediated Ag nanoparticles and analyzed the anti-bacterial activity by applying Gram-positive and Gram-negative bacteria separately for application in cotton textiles as an antibacterial coating. Moreover there is a lake of availability of textile industries based on AgNPs base research.

2. Experimental methods

2.1 Materials

In this research work, healthy and fresh leaves of *P. guajava* plant were collected from the tree, grown in front of BCSIR Dhaka Laboratories, Bangladesh. The tree was medium-sized; has leaves of 7–10 cm in length and 4–5 cm in width and remains green throughout the year. Analytical grade silver nitrate ($AgNO_3$) and sodium hydroxide (NaOH) were purchased from Merck, Germany (98% purity). Textile cotton and N95 mask fibers were obtained from local market of Bangladesh. For the preparation of leaf extract deionized water and Whatman no. 1 filter papers were used for erosion and filtration purpose. Moreover, for cleaning glassware (pipette, beaker, *etc.*) ethanol and distilled water were applied. Bacterial clinical isolations were generated by the Institute of National Analytical Research and Service (INARS), BCSIR.

2.2 Preparation of *P. guajava* leaf extract

For the preparation of leaf extract, fresh green leaves of *P. guajava* were taken, separated from the petiole and midrib, and washed with tap water thoroughly. The leaves were then washed further for several times to remove dust and surface contaminants using deionized water and hung for drying at room temperature (28 °C) for 1 hour. The dried leaves were sliced and cut into fine pieces using scissors. For preparing each batch of extract, 10 g of fine pieces of leaves were taken in a beaker with 100 mL of deionized water. The beaker was placed in a hot plate and stirred constantly at 400 rpm at 90 °C for 25 minutes to get leaf extract. This extract was filtered through Whatman filter paper for two times and kept at room temperature. Finally, the prepared aqueous leaf extract was poured into $AgNO_3$ solution in different concentrations. The rest of the extract was kept in the refrigerator at 4 °C covered by aluminum foil for further use.

2.3 Biosynthesis of silver nanoparticles

To synthesize silver nanoparticles, aqueous leaf extracts (1 mL of *P. guajava*) and 10 mL of $AgNO_3$ solution in different concentrations (10, 15, 20 and 25 mM) were taken in a beaker. The solution was placed in a hot plate; the temperature of the solution/mixture was raised to ~60 °C maintaining constant magnetic stirring for 10 minutes. Afterward, it was kept at room temperature for 2 hours where the reduction of Ag^+ ions to metallic Ag conversion was taken place. Finally, the solution was observed carefully, and without any pulsation, the color of the solution changed from light yellow to reddish brown which specifies the formation of AgNPs initially. A small portion of colored suspension was centrifuged at 10 000 rpm for 15 minutes to get powder material. Collected materials were washed with deionized water for several times to remove any impurities. It was then taken in a Petri dish and kept in an electric oven at 60 °C for 2 hours for drying. The dried powders were then annelid at 500 °C for 2 hours and stored in a desiccator for further use. Fig. 1 shows the whole procedure of synthesis of *P. guajava* leaf extract-mediated AgNPs.

2.4 Treatment of cotton and mask fibers

Cotton fiber from the local market may have dust, oil, hemicellulose and organic acids on its surface, so treatment is necessary to get anti-microbial cotton. At first, the cotton was washed with detergent to remove dust. Afterward, it was soaked

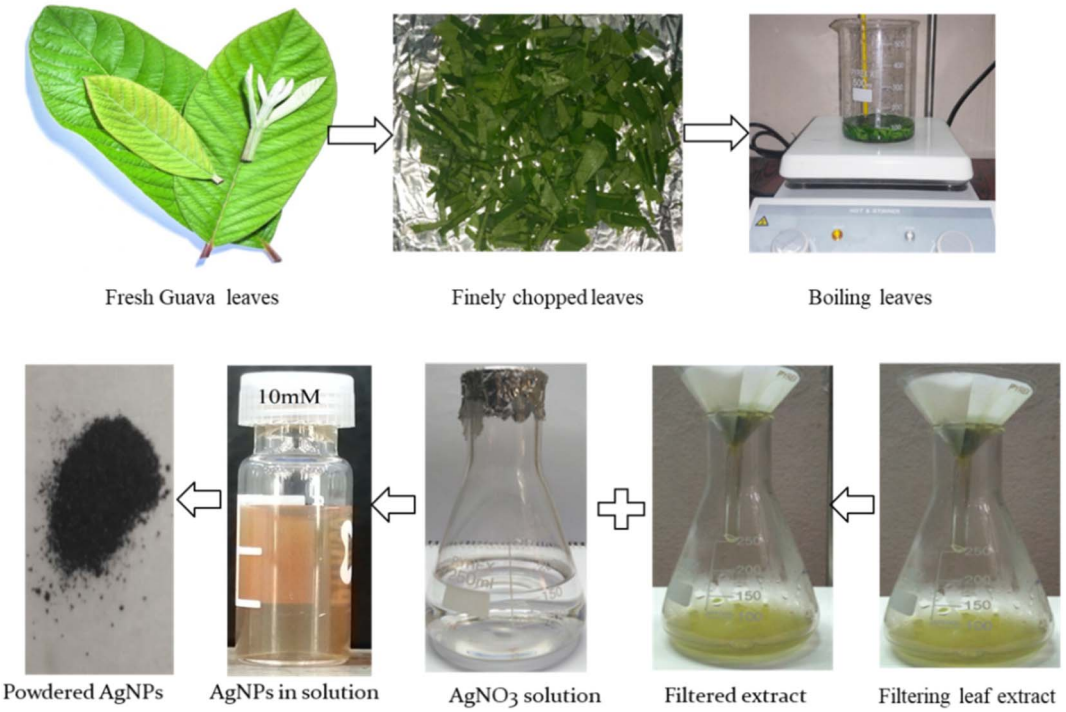

Fig. 1 Schematic representation for the synthesis of *P. guajava* leaf extract mediated AgNPs.

in a solution of ammonia and ethanol (4 : 6) for 10 hours in a dark room for oil removal. For alkali treatment, the fibers were washed thoroughly and dried in a vacuum oven at 40 °C for 24 hours. A 1 g cotton fiber was taken in a beaker and 30 mL NaOH solution was added so that the fiber emerged in the solution completely. The beaker was placed in a magnetic stirrer at 60 °C for 1 hour maintaining continuous stirring. Later, the cotton fiber was pulled out from the solution and washed three times before drying in the oven at 40 °C. However, fresh/new N95 mask fibers do not require any treatment and they were used as it is. Both cotton and N95 mask fibers were then treated by low-temperature RF oxygen plasma (10 min, 0.13 Torr, power input 100 W, RF-13.5 MHz) which was necessary to incorporate AgNPs into the fiber. Plasma modification generates active species on fiber surfaces thus it may used as a medium of antimicrobial agents.[11]

2.5 Preparation of AgNPs/cotton and AgNPs/N95 mask coating

A 1 g of plasma treated cotton fiber was dipped in 30 mL of aqueous solutions of synthesized *P. guajava* leaf extract-mediated AgNPs solution (10 mM). Similarly, 1 g of N95 mask fiber was soaked in 30 mL of aqueous solutions of synthesized AgNPs taken in another beaker. The beakers are then placed in a magnetic stirrer and stirred for 24 hours continually to get coated AgNPs/cotton and AgNPs/N95 mask. AgNPs can be incorporated homogeneously into the surface of the fibers because it becomes hydrophilic after plasma treatment. Finally, coated fibers were washed out with distilled water thoroughly to take out any residue and dried at 40 °C. The dried AgNPs/cotton and AgNPs/N95 masks were then reserved in a desecrator.

2.6 Instrumentation

The characteristic of synthesized AgNPs and coated fibers (cotton and mask) were investigated by different characterization techniques. The bioreduction of $AgNO_3$ in aqueous solution was observed with mixed plant extracts studies by using ultraviolet-visible near-infrared (UV-Vis-NIR) spectrophotometer (UV-2600, Shimadzu, Japan) ranging 200–800 nm. X-ray diffraction (XRD) (Rigaku Smart Lab, Japan) with Cu-Kα radiation (λ = 1.5406 Å) was used to confirm the crystallinity of AgNPs at room temperature. The scanning rate was 10° min^{-1}; power 40 kV at 40 mA and 0.02° step. A field emission scanning electron microscope (FE-SEM) (JSM-7610F, Japan) and energy dispersive X-ray (EDX) were used to study the surface morphology of AgNPs, AgNPs/cotton and AgNPs/mask composite and to identify the elemental composition of materials. Highly pure KBr powder was mixed with 1% (w/w) samples and then pressed into pellets to identify the bioactive functional group of AgNPs by Fourier transform infrared spectroscopy (FTIR, PerkinElmer, USA) recorded within 4000–350 cm^{-1}.

3. Results and discussion

3.1 Characterization of AgNPs

AgNPs have unique optical properties that help them to interact strongly with specific wavelengths of light.[21] To identify the formation of silver nanoparticles primarily the color of the solution was observed. After mixing the leaf extract with $AgNO_3$ for 2 two hours, due to surface plasmon resonance (SPR) the soft yellowish color of the solution has changed to brownish color which confirms the presence of AgNPs. Fig. 2 shows the color change observation of AgNPs solutions, the colors gave similar

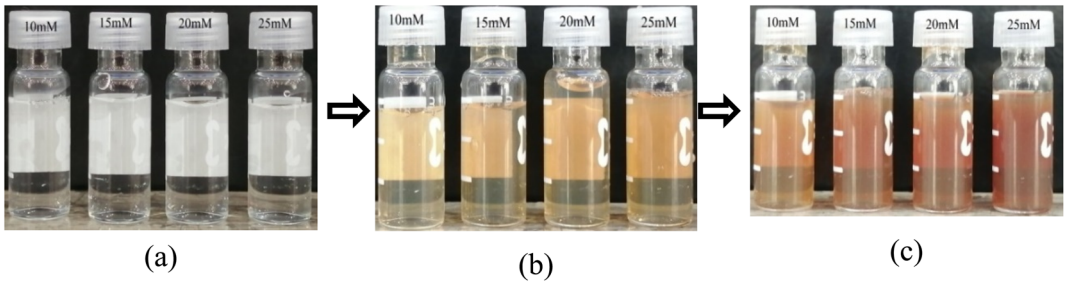

Fig. 2 Observation of color changes during synthesis of Ag NPs at different time intervals: (a) at the beginning (0.0 minutes), (b) after 60 minutes, and (c) after 120 minutes.

result with other previous research.[15] For further confirmation of the formation of NPs UV-Vis spectroscopic analysis was accomplished.

3.2 UV-vis spectroscopic analysis

UV-Vis spectroscopy is a firm, modest, sensitive and selective method used to identify different types of NPs initially. Moreover, no calibration is required to determine the particulate properties of the colloidal suspension.[22,23] Fig. 3(a) shows the UV-Vis absorption spectra of *P. guajava* leaf extract mediated AgNPs solution at wavelength 200–800 nm. The baseline data was taken using deionized water which is also referred as sample blank in this examination. The colored samples were diluted with deionized water and taken in the quartz cell of UV spectroscopy and the absorption peaks were found in the ultraviolet region at ~350–530 nm. The absorption peaks were determined at different concentrations of $AgNO_3$ salt and showed in Fig. 3(a). The intensity of absorption peaks increased with concentration however no shift change compared to leaf extract was observed.

In Fig. 3(b) and (c), the effect of time and temperature variation for 10 mM $AgNO_3$ solution was illustrated. It revealed that the absorption in the visible region is gradually increased with respect to time and temperature. From Fig. 3(b) the absorption intensity was red-shifted due to an increase in particle size with time interval which was confirmed by SPR intensity with help of the % reduction of Ag^+ to Ag^0. In addition, an increase in temperature favored the formation of leaf extract-mediated AgNPs and the wider peak of absorption indicates stable condition in Fig. 3(c). The free electron between the conduction band and the valence band moves and generate a range of absorption peak because of the mass oscillation of the electrons of the silver nanoparticles in the resonance with the optical wave at SPR.[24,25] The particle sizes, and surrounding chemical and electrical insulation are the main criteria of absorption of AgNPs.[26,27]

3.3 X-ray diffraction analysis

The structural properties of particles were analyzed by a conversant technique, XRD to get information about

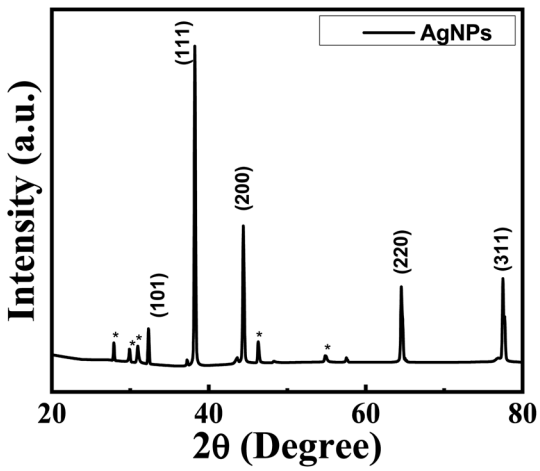

Fig. 4 XRD patterns of synthesized leaf extract mediated AgNPs.

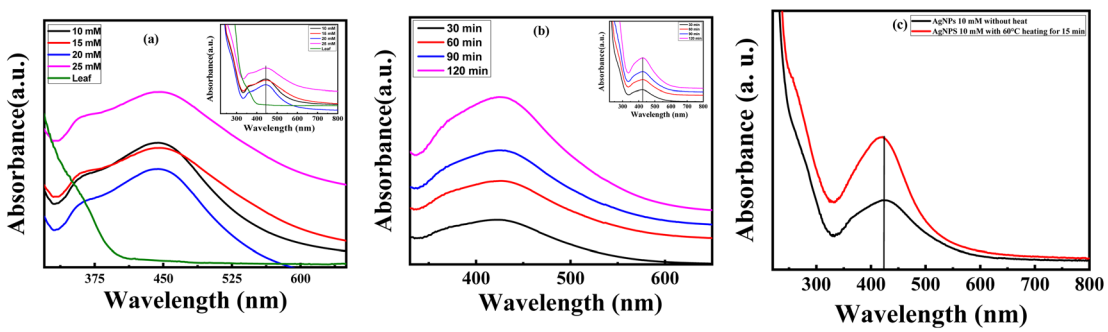

Fig. 3 UV-Vis absorption spectra of AgNPs (a) at different concentrations of $AgNO_3$ solution (b) at different time intervals for 10 mM $AgNO_3$ solution and (c) at different temperatures for 10 mM $AgNO_3$ solution.

crystallinity and phase formation. The XRD pattern with reflections at different angular positions of the synthesized AgNPs was shown in Fig. 4. The Bragg's peaks were observed at 2θ positions 32.99°, 39.21°, 44.39, 64.43° and 77.37° for (101), (111), (200), (220) and (311) crystal planes respectively. The formation of AgNPs were confirmed further by these characterization reflections. Also, the diffraction peaks of the XRD pattern correspond to the card (JCPDS No. 03-0921) which reflects those NPs are crystalline in nature.[28] The XRD pattern has confirmed that the synthesized samples were AgNPs with face-centered cubic crystal structure.[29]

Along with the characteristic peaks in the XRD pattern some * marked reflections also exist at 2θ (27.90°, 30.01°, 31.06, 46.34 and 54.97°) which were not known precisely. It may be due to the crystallization of bioorganic phases on the AgNPs surface that originates from the leaf extract[30] or due to $AgNO_3$ that was not reduced and remained in the sample slightly.[29] Many researchers also get similar patterns in XRD.[16–18]

The average crystallite size, D of the synthesized AgNPs were estimated from the diffractogram by using the Debye–Scherrer formula, $D = 0.9\lambda/\beta \cos\theta$, where λ and β are the wavelength of diffraction and full width at half maximum (FWHM) of a peak respectively.[31] The interplanar spacing between the atoms, d, was calculated using Bragg's law, and lattice constant, a, was determined.[32] The values of lattice parameters, d-spacing, FWHM, hkl value, and crystallite size at different angular position were demonstrated in Table 1.

From Table 1, it is seen that the D values are nearly identical for all the peaks and the average crystallite size obtained was ~22 nm. Thus, the XRD analysis of silver nanoparticles showed well-defined dimensions has fair agreement with the standard value for silver. Moreover, the lattice parameters, d-spacing, and hkl value calculated from the characteristic peaks of the synthesized sample match with reports of other researchers.[10,15]

3.4 Field emission scanning electron microscopy (FE-SEM) analysis

The surface morphology of guava leaf extract-mediated AgNPs were investigated by FE-SEM and illustrated in Fig. 5(a)–(d). The FE-SEM images showed a spherical shape for all the concentrations of $AgNO_3$ solutions. Fig. 5(d) showed distinct and homogeneous grain distribution; however, (10, 15, and 20 mM) $AgNO_3$ solution contains some agglomeration in Fig. 5(a)–(c).

Table 1 Structural parameters of synthesized leaf extract-mediated AgNPs

2θ (degree)	FWHM degree	Interplaner spacing, 'd' Å	$h\ k\ l$	Crystallite size 'D' nm	Lattice constant, 'a' Å
32.99	0.1538	2.7693	1 0 1	19.84	4.0315
39.21	0.148	2.3533	1 1 1	20.54	4.0956
44.39	0.1622	2.0462	2 0 0	20.96	4.0924
64.43	0.3582	1.4449	2 2 0	26.23	4.0868
77.37	0.5117	1.2329	3 1 1	19.90	4.0891

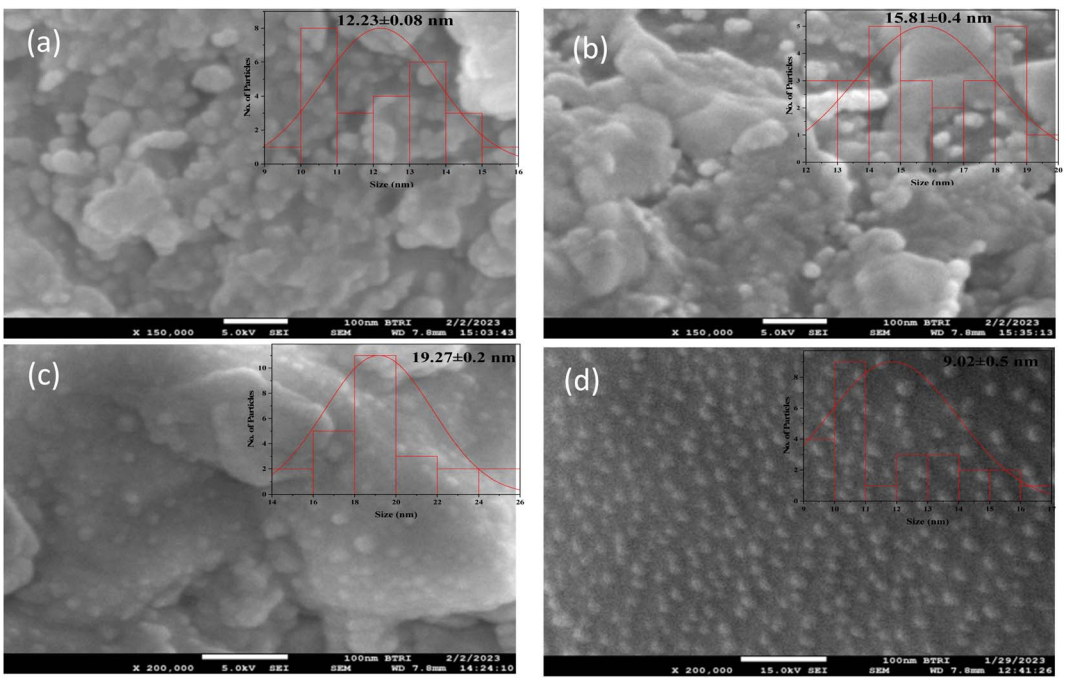

Fig. 5 FE-SEM images with grain size distribution of AgNPs for (a) 10 mM (b) 15 mM (c) 20 mM and (d) 25 mM of $AgNO_3$ solution.

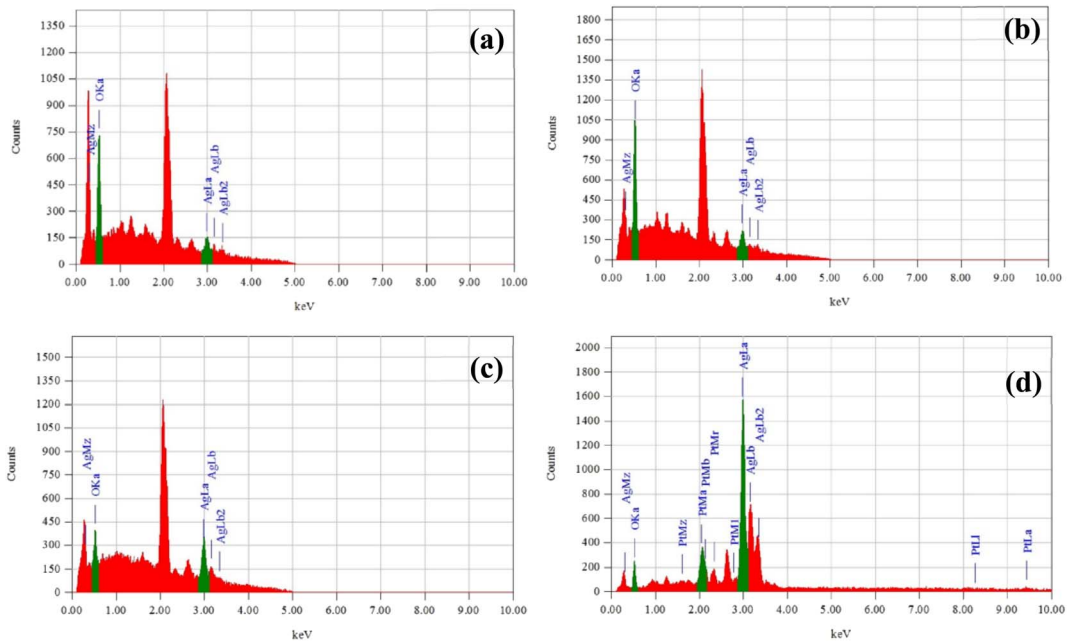

Fig. 6 EDX spectra of AgNPs for (a) 10 mM (b) 15 mM (c) 20 mM and (d) 25 mM of $AgNO_3$ solution.

Similar shape was found for ref. 33. The average grain size estimated in the range 12–19 nm for the variation of $AgNO_3$ solution against 10 : 1 leaf extract. The grain size measurement and distribution curve was calculated using Image J software. EDX spectra confirmed the presence of silver and oxygen shown in Fig. 6(a)–(d) also indicates the high purity of the synthesized AgNPs.[34]

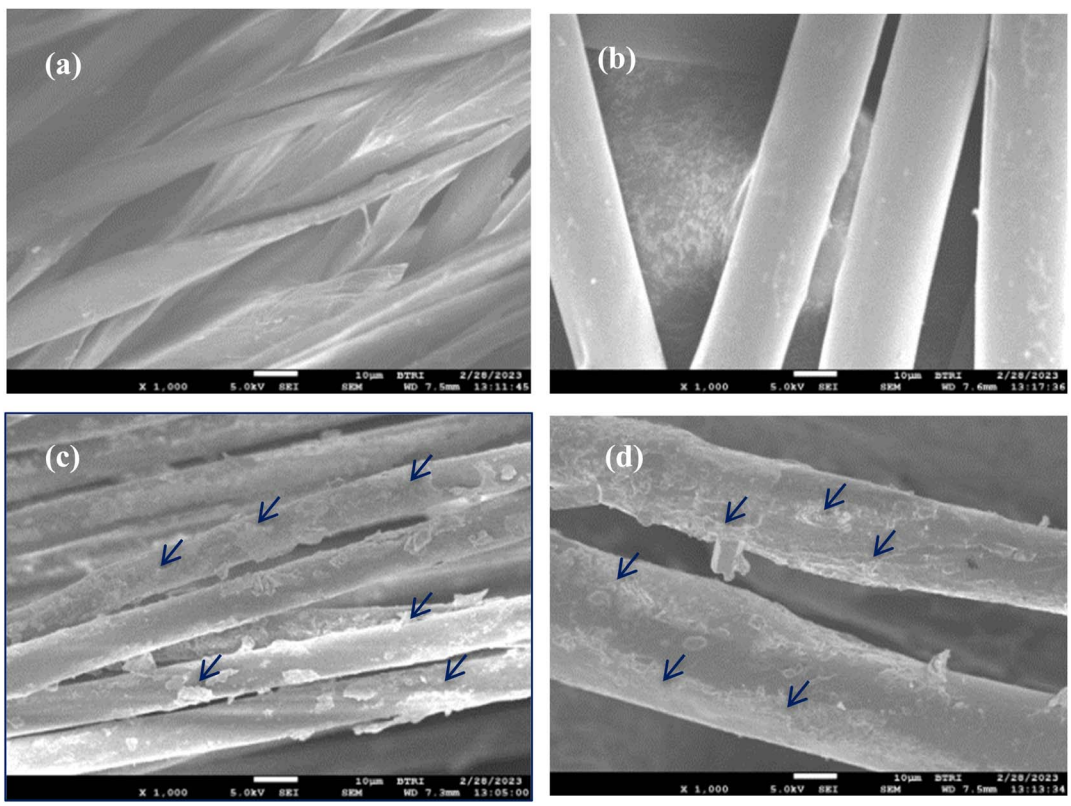

Fig. 7 FE-SEM micrograph of (a) treated cotton (b) treated N95 mask (c) AgNPs/treated cotton and (d) AgNPs/treated N95 mask.

The FE-SEM images of the treated cotton fiber and N95 mask surface are shown in Fig. 7(a) and (b) that sharper, clean, and pours free. Fig. 7(c) and (d) showed that the treated cotton fiber and N95 mask were coated homogeneously by AgNps. Oxygen plasma treatment creates more hydroxyl groups on the surface of the fibers that have stable conductive bonds with NPs, responsible for clinical isolation and antibiotic sensitivity.[20]

3.5 Fourier transforms infrared spectroscopy (FTIR) analysis

To detect functional group properties for NPs, FTIR is the most significant spectroscopic technique. FTIR spectra were employed to identify the photochemical elements in leaf extract-mediated AgNPs which are responsible for reducing and capping agents on Ag^+ ions to AgNPs. Those bioactive different functional groups produce effective NPs. In our research, guavas leave extract contains bioactive high polyphenolics acid molecules whose presence was found in FTIR spectra. The FTIR spectra of AgNPs with different functional groups was shown in Fig. 8. It revealed that the characteristic peak at 3445 cm^{-1} can be attributed to the –OH stretching indicating the capping and reducing agent.[8] In addition, –C–H stretching vibrations of alkane came from the carboxylic acid group at 2922 cm^{-1}. Highly conjugated carboxylic functional groups were found at 1383 cm^{-1} absorption band and the materialization oxygen group –C–O vibrations were confirmed at 1113 cm^{-1} respectively. The peak 613 cm^{-1} confirmed the formation of AgNPs where the –OH phenolic bond was shown matches with.[11] Thus, the fingerprint suggests that amid bonds belonging to aromatic, ethers and polyphenols are responsible bioactive elements that act as reducing and stabilizing agents for leaf extract-mediated AgNPs. The absorption peak was slightly shifted from guava leaf extract to AgNPs because of the formation of nanoparticles.

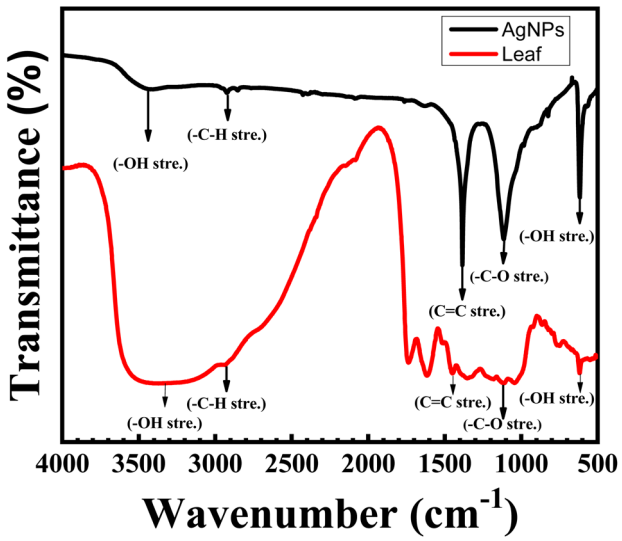

Fig. 8 FT-IR spectra of *P. guajava*-mediated AgNPs and leaf extract.

Table 3 Zone of inhibition (ZOI) for AgNPs solution against *E.coli* (Gram-negative) bacteria

AgNPs with different concentration of $AgNO_3$ solution (mM)	Zone of inhibition for Gram-negative (*E. coli*) (mm)
10	13.00
15	13.50
20	13.50
25	14.00

Table 2 FT-IR data

	Functional group at different characteristics absorptions (cm^{-1})				
Sample name	O–H (stretching)	C–H (alkane)	C=C (stretching)	–C–O (stretching)	O–H (stretching)
AgNPs	3445	2922	1383	1113	613
Leaf extract	3433	2924	1444	1126	617

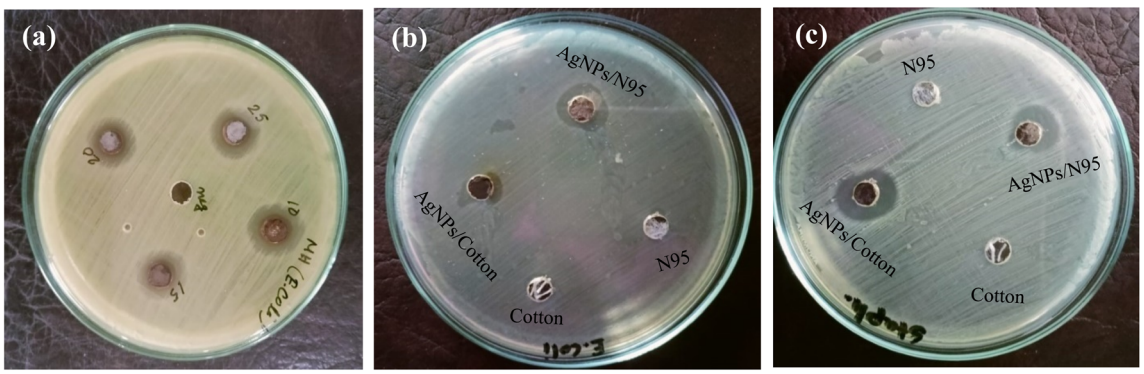

Fig. 9 Antibacterial activity of AgNPs (a) 10 mM, 15 mM, 20 mM, and 25 mM $AgNO_3$ solutions (b) AgNPs/treated cotton and AgNPs/treated N95 mask for *E. coli* (Gram-negative) bacteria and (c) AgNPs/treated cotton and AgNPs/treated N95 mask for *S. aureus* (Gram-positive) bacteria.

Table 4 Zone of inhibition for the *E. coli* (Gram-negative) bacteria and *S. aureus* (Gram-positive) bacteria

Name of bacteria	Zone of inhibition for AgNPs/treated cotton (mm)	Zone of inhibition for AgNPs/treated N95 mask (mm)
E. coli	11.50	15.00
S. aureus	18.00	14.50

Table 2 shows the different bioactive functional groups which confirm the formation of Ag^+ ions to AgNPs.[33,35]

3.6 Antibacterial activity

The antibacterial screening of NPs is one of the important studies to find an antibacterial agent. NPs can be considered effective antibacterial agent when it exhibits a significant zone of inhibition (ZOI) against bacteria.[36,37] A well disk diffusion method was applied for the measurement of zone of inhibition of *P. guajava*-assisted AgNPs.[38] To attune the optical density (OD 0.1) of bacteria in culture UV-visible spectrophotometer (JASCO V-600, Japan) was used. The sterile wipe of cotton was used to give a layer of bacterial pathogens on the well-cultured agar plate. Clinical pathogenic bacteria Gram-negative *Escherichia coli* (*E.coli*) and Gram-positive *Staphylococcus aureus* (*S. aureus*) were placed on a properly sterilized nutrient agar plate and kept in incubator at 37 °C for the whole night. In the experiment, the agar plate was prepared for each bacterium following the same procedure.

Afterward, AgNPs in various $AgNO_3$ concentration solutions were incorporated in the Gram-negative bacteria to confirm the activities of NPs. Also AgNPs/treated cotton and AgNPs/treated N95 masks were poured in Gram-negative bacteria (*E. coli*) and Gram positive (*S. aureus*) coated plate for testing its antibacterial activities in wet condition (Fig. 9). The samples were placed in oven for 2 hours so it may diffuse completely and then incubated for 24 hours at 37 °C. Finally, the diameters of restrictive zones were measured in mm.[38] The measurement values of zone of inhibition for each bacterial strain were shown in Tables 3 and 4.

In case of Gram-negative bacteria, the antimicrobial activity varied for each sample with different solution concentration. Due to the structure complexity of Gram-negative bacteria, the effective inhibition zone is greater in coated N95 mask than pure cotton. Cell wall thickness of Gram-negative has bigger width.[34] Also the coated AgNPs/treated cotton and AgNPs/treated N95 mask showed higher ZOI with strong antibacterial activity.

4. Conclusions

Silver nanoparticles were fabricated using aqueous leaf extract of *P. guajava* following green synthesis route. The reduction of silver ions from $AgNO_3$ to metallic Ag occurs due to leaf extract of *P. guajava*. The synthesized AgNPs were confirmed by observing the change of color initially and the absorbance peak at ~430 nm in UV-Vis spectroscopic analysis. Moreover, the XRD data revealed that it corresponds to the face-centered cubic structure of crystalline silver. Thus, the present method leads to the formation of silver nanoparticles with well-defined dimensions. The average crystalline size was estimated ~22 nm confirming the nanoparticle nature. However, FE-SEM analysis revealed that the material was formed in nano-dimension, with an average grain size ~12 nm. The particles were almost spherical in shape though their occurs has some agglomeration. In addition, the FTIR study showed the reduction of Ag^+ ions owing to the presence of biomolecules in the leaf extract, which acted as reducing as well as capping agents. Examination showed significant antibacterial activities of the synthesized AgNPs solution. The zone of inhibition in homogeneously coated treated cotton and N95 mask fiber showed a promising result against Gram-negative (*E. coli*) and Gram-positive (*S. aureus*) bacteria. The photo resistive properties of synthesized AgNPs signify their utility as an antibacterial coating in cotton textile applications.

Conflicts of interest

The authors declare that they have no conflict of interest.

Acknowledgements

Bangladesh Council of Scientific and Industrial Research (BCSIR), Dr Qudrat-I-Khuda Road, Dhanmondi, Dhaka-1205, Bangladesh.

References

1 S. Piretarighat, M. Ghannadnia and S. Baghshahi, *J. Nanostruct. Chem.*, 2019, **9**(1), 1–9.
2 I. Ijaz, E. Gilani, A. Nazir and A. Bukhari, *Green Chem. Lett. Rev.*, 2020, **13**(3), 223–245.
3 D. A. Kader, S. O. Rashid and K. M. Omer, *RSC Adv.*, 2023, **13**, 9963.
4 R. Khatun, M. S. A. Mamun, S. Islam, N. Khatun, M. Hakim, M. S. Hossain, P. K. Dhar and H. R. Barai, *Micromachines*, 2022, **13**(12), 2077.
5 J. R. Vega-Baudrit, S. M. Gamboa, E. R. Rojas and V. V. Martinez, *Biosens. Bioelectron.*, 2019, **5**, 5.
6 P. Velmurugan, M. Iydroose, S. Lee, M. Cho, J. Park, V. Balachandar and B. T. Oh, *Indian J. Microbiol.*, 2014, **54**, 196–202.
7 J. D. S. Newman and G. J. Blanchard, *Langmuri*, 2006, **22**(13), 5882–5887.
8 D. S. Sheny, J. Mathew and D. Philip, *Spectrochim. Acta, Part A*, 2011, **79**(1), 254–262.
9 D. Bose and S. Chattrjee, *Appl. Nanosci.*, 2016, **6**(6), 895–901.
10 S. P. Patil and P. M. Rane, *J. Basic Appl. Sci.*, 2020, **9**, 60.
11 M. J. Islam, M. T. Khatun, M. R. Rahman and M. M. Alam, *AIP Adv.*, 2021, **11**, 125223.
12 P. Somchaidee and K. Tedsree, *Adv. Nat. Sci.: Nanosci. Nanotechnol.*, 2018, **9**, 035006.

13 R. Saha, S. Karthik, P. M. R. S. A. Kumar, R. Suriyaprabha and V. Rajendran, *Prog. Org.*, 2018, **124**, 80–91.
14 J. Singh, V. Kumar, K. Kim and M. Rawat, *Environ. Res.*, 2019, **177**, 108569.
15 M. J. Islam, Kamaruzzaman, M. F. Hossain, M. A. Awal, M. R. Rahman and M. M. Alam, *AIP Adv.*, 2022, **12**(11), 115116.
16 M. Liu, D. Zhang, S. Chen and T. Wen, *J. Solid State Chem.*, 2016, **237**, 32–35.
17 C. Sharmila, R. Rajamani and C. S. Bellan, *Asian J. Pharm. Clin. Res.*, 2018, **11**(1), 341–345.
18 G. Venugopal, *Int. J. Bioassays*, 2017, **6**(7), 5441–5443.
19 L. B. Dama, P. P. Mane, A. V. Pathan, M. S. Chandarki, S. R. Sonawane, S. B. Dama, S. R. Chavan, R. P. Chondekar and A. S. Vinchurkar, *Sci. Res. Rep.*, 2016, **6**(2), 89–95.
20 A. Fakhri and M. Naji, *J. Photochem. Photobiol., B*, 2017, **167**, 58–63.
21 R. S. Zamel, B. K. Mohammed, A. S. Yaseen, H. T. Hussein and U. M. Nayef, *J. Res. Lepid.*, 2019, **50**(3), 82–95.
22 X. Huang, P. K. Jain, I. H. El-Sayed and M. A. El-Sayed, *Nanomedicine*, 2007, **2**, 681–693.
23 E. Tomaszewska, K. Soliwoda, K. Kadziola, B. Tkacz-Szczesna, G. Celichowski, M. Cichomski and J. Grobelny, *J. Nanomater.*, 2013, **2013**, 1–10.
24 M. Alam, *J. King Saud Univ., Sci.*, 2022, **34**, 102327.
25 R. Das, S. S. Nath, D. Chakdar, G. Gope and R. Bhattacharjee, *J. Nanotechnol.*, 2009, **5**, 1–6.
26 A. Taleb, C. Petit and M. P. Pileni, *J. Phys. Chem.*, 1998, **102**(12), 2214–2220.
27 S. Link and M. A. El-Sayed, *Annu. Rev. Phys. Chem.*, 2003, **54**(1), 331–366.
28 L. N. Khanal, K. R. Sharma, H. Paudyal and K. Parajuli, *J. Nanomater.*, 2022, **2022**(1), 1–11.
29 A. M. Awwad, N. M. Salem and A. O. Abdeen, *Int. J. Ind. Chem.*, 2013, **4**(1), 29.
30 A. Rautela, J. Rani and M. Debnath, *J. Anal. Sci. Technol.*, 2019, **10**, 5.
31 S. Islam, S. A. Satter, N. Khatun, M. S. Hossain, S. F. U. Farhad, P. Bala, S. Tabassum and A. Siddika, *J. Mol. Eng. Mater.*, 2019, 1–9.
32 S. Islam, N. Khatun, M. S. Habib, S. F. U. Farhad, N. I. Tanvir, M. A. A. Shaikh, S. Tabassum, D. Islam, M. S. Hossain and A. Siddika, *Heliyon*, 2022, **8**, e10529.
33 A. Jamaluddin and C. K. M. Faizal, *IIUM Eng. J.*, 2018, **19**(1), 178–184.
34 S. I. I. Abdel-Hafez, N. A. Nafady, I. R. Abdel-Rahim, A. M. Shaltout, J. Daròs and M. A. Mohamed, *3 Biotech*, 2016, **6**(2), 199.
35 V. Sreenivasulu, N. S. Kumar, M. Suguna, M. Asif, E. H. Al-Ghurabi, Z. X. Huang and Z. Zhen, *Int. J. Electrochem. Sci.*, 2016, 9959–9971.
36 S. Roy, I. Hasan and B. Guo, *Coord. Chem. Rev.*, 2023, **482**, 215075.
37 H. Huahg, A. Ali, Y. Liu, H. Xie, S. Ullah, S. Roy, Z. Song, B. Guo and J. Xu, *Adv. Drug Delivery Rev.*, 2023, **192**, 114634.
38 S. Shamaila, N. Zafar, S. Riaz, R. Sharif, J. Nazir and S. Naseem, *J. Nanomater.*, 2016, **6**(4), 71.